

First-principles study of the structures and energetics of stoichiometric brookite TiO_2 surfaces

Xue-Qing Gong* and Annabella Selloni

Department of Chemistry, Princeton University, Princeton, New Jersey 08544, USA

(Received 15 June 2007; published 10 December 2007)

First-principles density functional theory calculations at the generalized gradient approximation level are performed to investigate the structures and energetics of ten stoichiometric 1×1 low-index surfaces of brookite, the rarest and least understood of the natural polymorphs of titanium dioxide (TiO_2). For each surface, different possible terminations are considered, and their structural relaxations are analyzed. As a general trend, undercoordinated surface Ti atoms are found to relax inward so as to form TiO_x polyhedra with O atoms at the vertices, analogous to the TiO_6 octahedra of the bulk structure. For some surfaces, very large relaxations, involving several subsurface layers, are found to occur. From the computed surface formation energies, the relative stabilities of the different terminations are determined and found to be mainly related to the concentration of exposed coordinatively unsaturated metal (Ti) atoms. The equilibrium crystal shape of brookite TiO_2 is also determined, and the relative fraction of each exposed surface is estimated.

DOI: 10.1103/PhysRevB.76.235307

PACS number(s): 68.35.Bs, 71.15.Mb, 71.15.Nc

I. INTRODUCTION

Titanium dioxide (TiO_2) is one of the most extensively investigated metal oxide materials, largely because of its widespread use in many fields, e.g., catalysis, photocatalysis, solar energy conversion, and biomaterials.¹⁻⁴ Among the three main crystallographic forms of TiO_2 , namely, rutile (tetragonal, $P4_2/mnm$), anatase (tetragonal, $I4_1/amd$), and brookite (orthorhombic, $Pbca$), a great deal of attention has been focused on rutile and anatase,¹ whereas brookite has been rarely used and studied so far, mainly because of difficulties in preparing significant quantities of good quality material.^{5,6} Recently, however, efficient schemes to synthesize brookite TiO_2 with high purity have been devised, generating more and more interest in the physicochemical properties and possible applications of this TiO_2 polymorph.⁷⁻¹¹ For instance, a few comparative studies have already been carried out, suggesting that brookite may exhibit higher activity than rutile and anatase in photocatalysis and for catalytic reactions involving TiO_2 supported metal clusters.¹²⁻¹⁵ Since in all these applications, surfaces are primarily involved, a better characterization of the surfaces of brookite is clearly important for any future use of this material. In particular, the pronounced structure \leftrightarrow reactivity relationship that is observed for rutile and anatase TiO_2 surfaces strongly suggests that knowledge of the atomic structure of different brookite surfaces is essential for an understanding of the chemistry of this TiO_2 polymorph.^{1,16-19}

Theoretical studies based on first-principles electronic structure calculations have proven extremely useful in elucidating the relationship between atomic structure and physical and chemical properties of oxide surfaces.²⁰⁻²³ For brookite, only a few studies of this type are available, and its surface properties are still largely unknown.^{24,25} As a first step toward a better understanding of these surfaces, we have performed first-principles density functional theory (DFT) calculations to determine the structures and formation energies of ten different surfaces that appear to be frequently exposed by natural and synthetic brookite samples. In this paper, we present our findings, with particular focus on the relation

between surface structure and stability. The equilibrium crystal shape of brookite as determined through the Wulff construction is also reported.

This paper is organized as follows. Computational details are given in Sec. II. In Sec. III A, we compare the bulk structures of the three TiO_2 polymorphs, rutile, anatase, and brookite. The atomic structures and formation energies of all the investigated brookite surfaces are reported in the remaining part of Sec. III. Some general structural features of the relaxed surfaces as well as the predicted equilibrium crystal shape are discussed in Sec. IV, where a few concluding remarks are also given.

II. COMPUTATIONAL DETAILS

The total energy DFT calculations have been carried out within the generalized gradient approximation using the PWSCF code included in the QUANTUM-ESPRESSO package.^{26,27} Electron-ion interactions were described by ultrasoft pseudopotentials,²⁸ with electrons from O $2s$, $2p$ and Ti $3s$, $3p$, $3d$, $4s$ shells explicitly included in the calculations. Plane-wave basis set cutoffs for the smooth part of the wave functions and the augmented density were 25 and 200 Ry, respectively. For calculations on bulk brookite, a $2 \times 3 \times 3$ k -point mesh was used to sample the Brillouin zone corresponding to the primitive unit cell, which contains eight TiO_2 units. The optimized a , b , and c bulk lattice parameters are 9.140 (9.166), 5.407 (5.436), and 5.176 (5.135) Å, respectively, in close agreement with the experimental values (between parentheses).²⁹

Brookite TiO_2 surfaces were modeled using periodic slab geometries and the vacuum between slabs was ~ 10 Å. For each surface, the primitive (1×1) surface cell was considered, and, depending on its dimensions, a different k -point mesh was used to sample the corresponding surface Brillouin zone. Specifically, the following k -point meshes were used: $2 \times 1 \times 1$, for brookite $\text{TiO}_2(110)$, (010), (210), and (120); $1 \times 2 \times 1$, for brookite $\text{TiO}_2(001)$, (101), and (111); $1 \times 1 \times 1$ for brookite $\text{TiO}_2(011)$ and (121); $2 \times 2 \times 1$ for brookite $\text{TiO}_2(100)$. During structural optimizations, all the atoms of

TABLE I. Calculated surface formation energies γ of different brookite TiO_2 surfaces. For some surfaces, different terminations (types) are considered; values in bold indicate the most stable termination. For the surfaces exposed on the computed crystal shape, the relative fraction areas are given.

Surface	(100)		(010)		(001)		(110)		
	I	II	I	II	I	I-R	II	I	II
γ (J m^{-2})	0.93	0.88	1.21	0.77	1.18	0.62	0.87	0.99	0.85
Figure	2(a)	2(b)	3(a)	3(b)	4(a) and 4(c)	4(e)	4(b) and 4(d)	5(a)	5(b)
Fraction	2%		7%		18%				
Surface	(011)	(101)	(111)				(210)	(120)	(121)
			I	II	III	IV			
γ (J m^{-2})	0.74	0.87	0.72	0.77	0.91	1.12	0.70	0.82	1.04
Figure	6	7	8(a)	8(b)			9	10	
Fraction	4%	2%	34%				33%		

the slabs were allowed to move (force threshold = $0.05 \text{ eV}/\text{\AA}$).

In order to estimate surface formation energies, for each termination, slabs with different numbers of layers were constructed. The computed total energies of the slabs, together with their corresponding numbers of TiO_2 units, were then fitted into the following equation to extrapolate the surface formation energy γ ,

$$E_{total} = 2\gamma A + nE_{\text{TiO}_2}. \quad (1)$$

Here, E_{total} is the total energy of the slab, n is the number of TiO_2 units in the slab, E_{TiO_2} is the energy of one TiO_2 unit in bulk brookite, and A is the exposed area of one side of the slab (slabs exposing two identical surfaces were used). The calculated values of γ for all the investigated surfaces are summarized in Table I and will be discussed in the following.

III. RESULTS

A. Brookite bulk structure

The bulk structures of rutile, anatase, and brookite TiO_2 are shown in Fig. 1. In all these three polymorphs, each Ti binds with six O and each O with three Ti; therefore, their structures can be described in terms of TiO_6 octahedra, with Ti at the center and O at the vertices. Alternatively, the TiO_2 bulk structure can also be analyzed in terms of OTi_3 units,²⁵ but the extension of this type of description to surfaces—which are the main focus of the present investigation—is less straightforward. For rutile, the TiO_6 octahedra along the **a**, [100], and **b**, [010], directions share vertices, while those along the **c**, [001], direction share edges. For anatase, the TiO_6 octahedra share edges along all the three directions, though in a zigzag way. For brookite, the structure is more complicated: Along the **a** and **b** directions, both vertex sharing (between gray and yellow/blue octahedra) and edge shar-

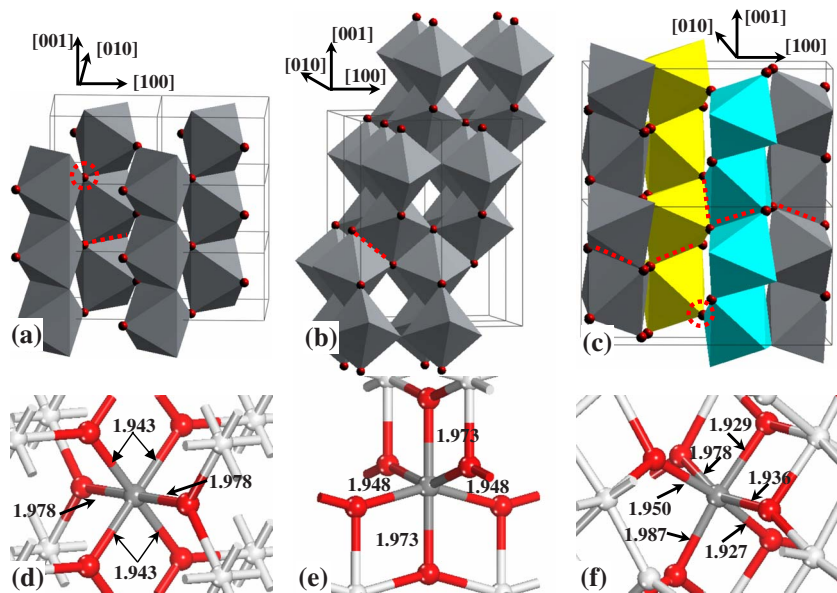


FIG. 1. (Color online) Bulk structures of rutile (a), anatase (b), brookite (c), showing the linking of TiO_6 octahedra through edges and vertices (a few of these have been indicated by dashed red lines and circles, respectively). The octahedra are in gray, except the middle two of brookite, which are colored yellow and light blue. The coordinations of the Ti atoms at the center of the TiO_6 octahedra in rutile, anatase, and brookite are shown in (d), (e), and (f), respectively. The calculated bond distances are given in \AA . The O atoms are in red and Ti in gray, and the atoms not included in the octahedra are white.

ing (between yellow and blue octahedra) occur, so that both rutile and anatase characteristics are present; along the c direction, the TiO_6 octahedra share edges, in a way very similar to rutile. Note also that while in anatase and rutile each Ti has two long (apical) and four short (equatorial) bonds with the neighboring O atoms [Figs. 1(d) and 1(e)], the six Ti-O bonds are all different in the case of brookite [Fig. 1(f)].

From our calculation of the surface energies via Eq. (1), the bulk energy E_{TiO_2} can also be determined. In this way, we estimate E_{TiO_2} (brookite) = -181.217 Ry per TiO_2 unit to be compared to E_{TiO_2} (anatase) = -181.226 Ry and E_{TiO_2} (rutile) = -181.212 Ry from analogous calculations for anatase²³ and rutile¹⁶ slabs. As expected on the basis of the structural analysis given above, the stability of brookite is intermediate between those of anatase and rutile, as found also experimentally.³⁰ However, the ordering of the computed stabilities is opposite with respect to the experiment,³⁰ a fact that, for the case of anatase vs rutile, has been already reported by previous DFT studies.^{16,31} This puzzling result does not seem to depend on the choice of the DFT exchange-correlation functional: Indeed, it has been recently confirmed by an extensive computational study where several different functionals, including hybrid functionals, have been used.³² In spite of this difficulty, DFT calculations have proven capable of correctly predicting relaxed structures and relative stabilities of different rutile and anatase TiO_2 surfaces, as well as the equilibrium crystal shapes of the rutile anatase TiO_2 polymorphs.^{1,16,33,34}

B. Brookite surface structures

The similarities between the bulk structure of brookite and those of the other two TiO_2 polymorphs are also reflected in their surface structures. For most of the investigated brookite surfaces, we have identified a rutile and/or anatase surface showing similar structural features. The similarities among the surfaces of the three TiO_2 polymorphs are summarized in Table II and will be described in more detail in the following.

1. Brookite $\text{TiO}_2(100)$

The brookite $\text{TiO}_2(100)$ surface has two possible terminations, which we denote as type I and type II (see Fig. 2). Important structural parameters before and after optimization are listed in Table III. Both types I and II surfaces expose

TABLE II. Low-index brookite TiO_2 surfaces and structurally similar surfaces in rutile and anatase.

Brookite	(100)	(010)	(001)	(110)	(101)	(210)
Rutile		(001)	(011)		(111)	
Anatase	(112)	(110)		(312)		(101)

fully coordinated sixfold Ti (Ti_{6c}) and threefold O (O_{3c}) atoms, as well as coordinatively unsaturated (cus) fivefold Ti (Ti_{5c}) and twofold O (O_{2c}) atoms. The (100) slab shows stacks of trapezoidally shaped Ti_2O_4 units along the $[100]$ direction (see Fig. 2). For each trapezoid, the two O-O pairs are on the parallel sides, while the two O-Ti-O trimers are on the two nonparallel sides. The trapezoids on adjacent layers along $[100]$ have two different orientations; e.g., the shorter of the two parallel sides can be “up” or “down,” and the two different (100) terminations correspond to one or the other orientation of the trapezoids in the outer layer. On both types I and II terminations, relaxations are more important for the cus atoms. For the type I surface, for example, the bonds between one Ti_{5c} and two coordinating O_{2c} atoms ($\text{Ti}_{5c}1\text{-O}_{2c}1$ and $\text{Ti}_{5c}1\text{-O}_{2c}2$) decrease from 1.929 and 1.927 Å on the bulk-truncated surface to 1.788 and 1.883 Å, respectively. In addition, the Ti_{5c} atoms tend to move toward each other along the $[001]$ direction in such a way that the “tips” of the saw-toothed surface appear to be somewhat sharper than those before relaxation. Accordingly, the bonds between one Ti_{5c} and the two O_{3c} on the same side of the tip ($\text{Ti}_{5c}1\text{-O}_{3c}2$, $\text{Ti}_{5c}1\text{-O}_{3c}3$) increase from 1.950 and 1.987 Å to 2.038 and 2.110 Å, respectively, while the distance between the Ti_{5c} and the O_{3c} on the other side of the tip ($\text{Ti}_{5c}1\text{-O}_{3c}4$) decreases from 1.978 to 1.811 Å. Moreover, the bond angles for $\text{Ti}_{5c}1$ ($\text{O}_{2c}1\text{-Ti}_{5c}1\text{-O}_{3c}3$ and $\text{O}_{2c}2\text{-Ti}_{5c}1\text{-O}_{3c}2$) are also remarkably reduced (see Table III). Altogether, the relaxation tends to embed the exposed Ti_{5c} toward the center of a TiO_5 polyhedron. The computed surface formation energies for types I and II brookite $\text{TiO}_2(100)$ are very similar, 0.93 and 0.88 J m^{-2} , respectively. These values are similar to the surface formation energy of anatase $\text{TiO}_2(112)$, ~ 0.9 J m^{-2} , which the structures of the brookite $\text{TiO}_2(100)$ closely resembles.²³ The relaxations at the (100) brookite and (112) anatase surfaces are also very similar; for instance, on anatase $\text{TiO}_2(112)$, the top $\text{O}_{2c}\text{-Ti}_{5c}$ bonds also shrink remarkably and two neighboring Ti_{5c} move toward each other upon relaxation.

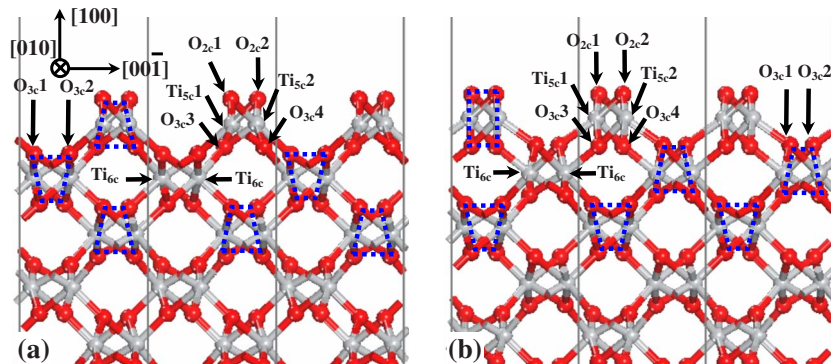


FIG. 2. (Color online) Optimized structures of brookite $\text{TiO}_2(100)$: (a) type I and (b) type II terminations. Three surface cells are shown, with cell boundaries being indicated by thin lines in gray. Dashed blue quadrangles indicate Ti_2O_4 units. In this and all following figures, the O atoms are in red and Ti in gray.

TABLE III. Structural parameters of bulk-truncated (before) and optimized (after) brookite $\text{TiO}_2(100)$; surface atoms are labeled as in Fig. 2.

	Brookite $\text{TiO}_2(100)$					
	Type I		Type II			
	Before	After	Before	After	Before	After
$\text{Ti}_{5c}1\text{-O}_{2c}1$ (Å)	1.929	1.788	$\text{Ti}_{5c}1\text{-O}_{2c}1$ (Å)	1.987	1.799	
$\text{Ti}_{5c}1\text{-O}_{2c}2$ (Å)	1.927	1.883	$\text{Ti}_{5c}1\text{-O}_{2c}2$ (Å)	1.978	1.883	
$\text{Ti}_{5c}1\text{-O}_{3c}2$ (Å)	1.950	2.038	$\text{Ti}_{5c}1\text{-O}_{3c}2$ (Å)	1.936	1.957	
$\text{Ti}_{5c}1\text{-O}_{3c}3$ (Å)	1.987	2.110	$\text{Ti}_{5c}1\text{-O}_{3c}3$ (Å)	1.929	2.184	
$\text{Ti}_{5c}1\text{-O}_{3c}4$ (Å)	1.978	1.811	$\text{Ti}_{5c}1\text{-O}_{3c}4$ (Å)	1.927	1.795	
$\text{O}_{2c}1\text{-Ti}_{5c}1\text{-O}_{3c}3$ (deg)	172.157	167.093	$\text{O}_{2c}1\text{-Ti}_{5c}1\text{-O}_{3c}3$ (deg)	172.157	173.919	
$\text{O}_{2c}2\text{-Ti}_{5c}1\text{-O}_{3c}2$ (deg)	171.270	161.849	$\text{O}_{2c}2\text{-Ti}_{5c}1\text{-O}_{3c}2$ (deg)	160.968	143.751	

2. Brookite $\text{TiO}_2(010)$

The bulk-truncated brookite $\text{TiO}_2(010)$ also has two possible terminations, both exposing cus O_{2c} and fourfold Ti_{4c} , as well as saturated O_{3c} and Ti_{6c} atoms. The corresponding optimized structures are shown in Fig. 3, while structural parameters (bond lengths and angles) are given in Table IV. For the type I surface [Fig. 3(a)], the surface largely keeps the original saw-toothed conformation upon relaxation. However, the two O_{2c} ($\text{O}_{2c}1$ and $\text{O}_{2c}2$) binding with Ti_{4c} undergo significant outward relaxations (~ 0.1 and ~ 0.5 Å, respectively), whereas the Ti_{4c} atoms are relaxed inward (~ 0.1 Å). As a result, the TiO_4 units achieve a better tetrahedral configuration with the Ti_{4c} close to the center. The calculated surface energy is 1.21 J m^{-2} .

For the type II brookite $\text{TiO}_2(010)$ [Fig. 3(b)], relaxation gives rise to more substantial structural changes and significant bond rearrangements, which also involve atoms a few layers below the surface. In particular, the exposed Ti_{6c} atoms on the bulk-truncated surface break their bonds with the O_{3c} below ($\text{Ti}_{6c}\text{-O}_{3c}3$; $\text{O}_{3c}3$, in fact, becomes twofold after relaxation) and rise by more than 0.5 Å. Accordingly, the O_{2c} atoms binding with these Ti_{6c} also relax outward by about 0.4 Å, whereas the top Ti_{4c} atoms relax inward. As a result, the optimized type II brookite $\text{TiO}_2(010)$ surface exposes newly formed Ti_{5c} (labeled as Ti_{6c} in Fig. 3) besides other cus atoms, and the outmost Ti_{4c} atoms are well at the center of TiO_4 tetrahedra. Due to this large surface relaxation, the type II surface, with a computed formation energy of 0.77 J m^{-2} , is much more stable than the type I termination.

3. Brookite $\text{TiO}_2(001)$

Figures 4(a) and 4(b) show the two possible structures of bulk-truncated brookite $\text{TiO}_2(001)$, while the calculated

structural parameters before and after relaxation are listed in Table V. The only difference between the two terminations is that the type II surface [Fig. 4(b)] has two less TiO_2 units compared to type I [Fig. 4(a)]. Accordingly, the type I surface appears to be rather flat, while the type II surface looks more undulate. The type I (001) surface exposes cus fourfold Ti (two per unit cell) and twofold oxygens, as well as saturated Ti_{6c} and O_{3c} , while type II (001) surface exposes cus fivefold Ti (four per unit cell) and twofold oxygens.

Type II brookite $\text{TiO}_2(001)$ undergoes significant structural changes upon relaxation [Fig. 4(d)]. For instance, the topmost Ti_{5c} atoms ($\text{Ti}_{5c}1$ and $\text{Ti}_{5c}2$) move toward each other along the $[100]$ direction and break their bonds with the subsurface O_{3c} [indicated by dashed arrows in Fig. 4(d)], therefore becoming fourfold coordinated. The O_{2c} atoms bonding with the topmost Ti_{5c} also move substantially. The resulting surface formation energy is 0.87 J m^{-2} .

For the type I (001) surface, two different structures have been identified. A structure quite similar to the bulk-truncated one and with a surface formation energy of 1.18 J m^{-2} is obtained by straightforward optimization of the bulk-truncated surface [Fig. 4(c)]. Using a somewhat more elaborate optimization procedure, however, an additional, more stable 1×1 reconstructed surface, with a formation energy as low as 0.62 J m^{-2} , is found [see Fig. 4(e)]. By comparing Fig. 4(e) to the “local minimum” structure in Fig. 4(c), it appears that the reconstructed surface involves a few Ti-O bond breaking and rearrangement processes: The sub-surfaces O_{3c} specified by dashed arrows break their bonds with the two exposed Ti_{6c} ($\text{Ti}_{6c}1$ and $\text{Ti}_{6c}2$) and move toward each other along the directions shown in Fig. 4(e). Meanwhile, the exposed O_{3c} ($\text{O}_{3c}1$ and $\text{O}_{3c}2$) break their bonds with the subsurface Ti_{6c} and rise above the Ti_{4c} atoms. As a result, the reconstructed type I brookite $\text{TiO}_2(001)$ exposes

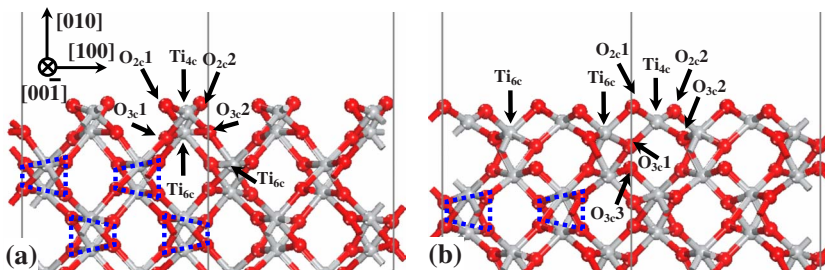


FIG. 3. (Color online) Optimized structures of brookite $\text{TiO}_2(010)$ with type I (a) and type II (b) terminations. Atoms in two surface cells are shown (cell boundaries are thin lines in gray). Dashed blue quadrangles indicate Ti_2O_4 units.

TABLE IV. Structural parameters of bulk-truncated (before) and optimized (after) brookite $\text{TiO}_2(010)$; different surface atoms are labeled as in Fig. 3.

	Brookite $\text{TiO}_2(010)$					
	Type I		Type II			
	Before	After	Before	After	Before	After
$\text{Ti}_{4c}\text{-O}_{2c}1$ (Å)	1.987	1.825	$\text{Ti}_{4c}\text{-O}_{2c}1$ (Å)	1.929	1.816	
$\text{Ti}_{4c}\text{-O}_{2c}2$ (Å)	1.929	1.824	$\text{Ti}_{4c}\text{-O}_{2c}2$ (Å)	1.987	1.858	
$\text{Ti}_{4c}\text{-O}_{3c}1$ (Å)	1.978	1.824	$\text{Ti}_{4c}\text{-O}_{3c}1$ (Å)	1.936	1.789	
$\text{Ti}_{4c}\text{-O}_{3c}2$ (Å)	1.927	1.805	$\text{Ti}_{4c}\text{-O}_{3c}2$ (Å)	1.950	1.827	
$\text{O}_{2c}1\text{-Ti}_{4c}\text{-O}_{2c}2$ (deg)	172.157	152.817	$\text{Ti}_{6c}\text{-O}_{3c}3$ (Å)	1.927	2.410	
			$\text{O}_{2c}1\text{-Ti}_{4c}\text{-O}_{2c}2$ (deg)	172.157	137.486	

four newly formed Ti_{5c} atoms besides the two Ti_{4c} , and the four O_{3c} involved in the reconstruction become twofold. All the exposed Ti atoms (Ti_{4c} and Ti_{5c}) are symmetrically surrounded by O_{2c} and O_{3c} , so as to be located at the center of tetrahedra and pentahedra formed by these O atoms.

4. Brookite $\text{TiO}_2(110)$

The brookite $\text{TiO}_2(110)$ surface has several possible terminations. Among them, we have studied the two that are likely to be the most stable on the basis of the type and density of exposed undercoordinated atoms. Their relaxed structures are shown in Fig. 5, and the relevant structural parameters are listed in Table VI. Both terminations look like

vicinal surfaces, with terraces separated by step edges. O_{2c} and fourfold Ti (Ti_{4c}) atoms are exposed at the step edges, while O_{3c} , O_{2c} , Ti_{6c} , and Ti_{5c} occur at the terraces. The optimized structures show large relaxations, especially at the step edges, where the exposed O_{2c} relax outward, while the cus Ti atoms relax inward. The calculated formation energies are 0.99 and 0.85 J m^{-2} for the types I and II terminations, respectively. This difference can be explained by the fact that the O_{2c} ($\text{O}_{2c}2$) at the step edge of the type I surface [Fig. 5(a)] is quite close to a nearby terrace O_{2c} (distance = 2.804 Å), suggesting a large repulsion between them.²³ This unfavorable interaction does not exist on the type II (110) surface.

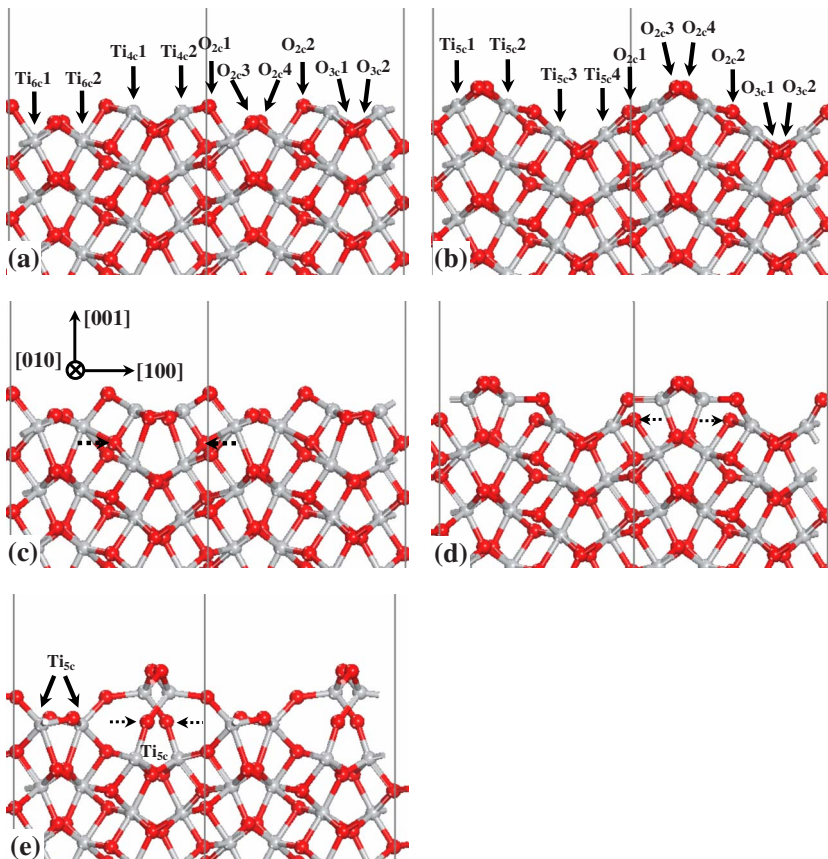


FIG. 4. (Color online) Brookite $\text{TiO}_2(001)$ with type I (left panel) and type II (right panel) terminations before (a) and (b) and after (c) and (d) relaxation, or following reconstruction (e). The atoms in two surface cells are shown (cell boundaries are thin lines in gray). The dashed arrows in (c) and (e) show the displacements of the O atoms in the reconstruction.

TABLE V. Structural parameters of *unreconstructed* brookite $\text{TiO}_2(001)$ before and after optimization. O_d is the O specified by dashed arrow (see Fig. 4).

Brookite $\text{TiO}_2(001)$					
Type I	Type I		Type II		
	Before	After	Before	After	
$\text{Ti}_{4c}1\text{-O}_{2c}2$ (Å)	1.936	1.781	$\text{Ti}_{5c}1\text{-O}_{2c}1$ (Å)	1.936	1.921
$\text{Ti}_{4c}1\text{-O}_{3c}1$ (Å)	1.978	1.913	$\text{Ti}_{5c}1\text{-O}_{2c}3$ (Å)	1.978	1.862
$\text{Ti}_{4c}1\text{-O}_{3c}2$ (Å)	1.950	1.833	$\text{Ti}_{5c}1\text{-O}_{2c}4$ (Å)	1.950	1.804
$\text{Ti}_{4c}1\text{-O}_d$ (Å)	1.929	1.770	$\text{Ti}_{5c}1\text{-O}_d$ (Å)	1.927	2.331
$\text{O}_{2c}2\text{-Ti}_{4c}1\text{-O}_{3c}1$ (deg)	199.032	145.459	$\text{O}_{2c}1\text{-Ti}_{5c}1\text{-O}_{2c}3$ (deg)	160.968	142.637

5. Brookite $\text{TiO}_2(011)$

The atomic arrangement on the brookite $\text{TiO}_2(011)$ surface is quite irregular. In Fig. 6, we show the optimized structure of the (011) termination that is considered in this work, while the corresponding structural parameters are listed in Table VII. This surface exposes cus Ti_{4c} , Ti_{5c} , and O_{2c} , as well as saturated Ti_{6c} and O_{2c} atoms. Other possible (011) terminations exhibit species such as one-fold O and three-fold Ti atoms, which are expected to have very high energies. Upon relaxation, all the exposed Ti and O atoms undergo rather large displacements, while keeping their original coordination numbers. As found on other TiO_2 surfaces, the cus Ti_{4c} and Ti_{5c} atoms relax inward, while saturated Ti_{6c} atoms relax outward. The computed formation energy of the relaxed brookite $\text{TiO}_2(011)$ surface is 0.74 J m^{-2} .

6. Brookite $\text{TiO}_2(101)$

The low-index (101) surface of brookite has several possible terminations. Among them, we have chosen the one that seems likely to give the lowest formation energy [see Fig. 7(a)]. This bulk-truncated (101) surface exposes cus Ti_{4c} , Ti_{5c} , and O_{2c} atoms, as well as saturated Ti_{6c} and O_{3c} atoms. The relaxed structure is shown in Fig. 7(b), and some structural parameters are given in Table VIII. It appears that the Ti_{4c} and Ti_{6c} ($\text{Ti}_{6c}1$) atoms are relaxed inward and outward, respectively, while the Ti_{5c} and O_{2c} atoms undergo only minor displacements. Most notably, the displacement of the surface O_{3c} atom is huge: This atom rises by $\sim 0.7 \text{ \AA}$, breaking its bond with the subsurface Ti atom ($\text{Ti}_{6c}2$). In the resulting configuration, the two Ti_{4c} atoms ($\text{Ti}_{4c}1$ and $\text{Ti}_{4c}2$) are then located close to the center of TiO_4 tetrahedra involving the raised O_{3c} (in fact, the O_{3c} and $\text{Ti}_{6c}2$ become twofold and

fivefold, respectively). The resulting formation energy is rather high, 0.87 J m^{-2} .

7. Brookite $\text{TiO}_2(111)$

Brookite $\text{TiO}_2(111)$ also looks irregular and complicated, and has various possible terminations. Since it is hard to predict their relative stabilities, we examined as many as four different terminations. They all expose cus Ti_{4c} , Ti_{5c} , and O_{2c} atoms and differ from each other mainly in the concentration and coordination number of exposed Ti atoms. Type I termination has one Ti_{4c} and three Ti_{5c} per unit cell [see Fig. 8(a)], type II has six Ti_{5c} [see Fig. 8(b)], type III has one Ti_{4c} and four Ti_{5c} , and type IV has seven Ti_{5c} (types III and IV are not shown). After optimization, all the four relaxed surfaces (not shown) largely keep their original conformations. However, they have very different surface energies, 0.72 , 0.77 , 0.91 , and 1.12 J m^{-2} , for types I, II, III, and IV, respectively. These relative stabilities are mainly determined by the concentration of cus Ti atoms. From the calculated surface energies, we conclude that the type I structure is the most likely to occur at brookite $\text{TiO}_2(111)$.

8. Brookite $\text{TiO}_2(210)$

This surface corresponds to the terrace part of the vicinal brookite $\text{TiO}_2(110)$ surface. The slab exposing the (210) surface can be viewed as a stack of Ti_2O_4 trapezoids [see Fig. 9(a)], similar to the (100), (010), and (110) slabs. More importantly, the structure of the brookite (210) surface is very close to that of the most stable anatase surface, namely, anatase (101) (Ref. 23): It has the same type of building block [indicated as a dashed blue rectangle in Figs. 9(b) and 9(c)], which consists of cus Ti_{5c} and O_{2c} atoms, as well as satu-

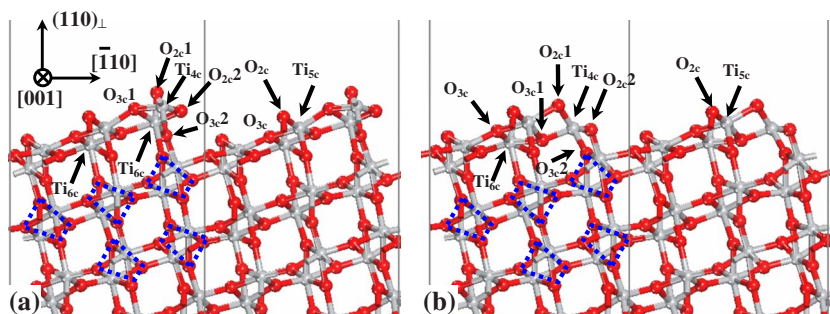


FIG. 5. (Color online) Optimized structures of brookite $\text{TiO}_2(110)$: (a) type I and (b) type II terminations. Atoms in two surface cells are shown (cell boundaries are thin lines in gray). Dashed blue quadrangles indicate Ti_2O_4 units. $(110)_\perp$ denotes the normal of the (110) surface.

TABLE VI. Structural parameters of bulk-truncated (before) and optimized (after) brookite $\text{TiO}_2(110)$; surface atoms are labeled as in Fig. 5.

	Brookite $\text{TiO}_2(110)$					
	Type I		Type II			
	Before	After	Before	After		
$\text{Ti}_{4c}\text{-O}_{2c}1$ (Å)	1.929	1.828	$\text{Ti}_{4c}\text{-O}_{2c}1$ (Å)	1.929	1.848	
$\text{Ti}_{4c}\text{-O}_{2c}2$ (Å)	1.987	1.796	$\text{Ti}_{4c}\text{-O}_{2c}2$ (Å)	1.987	1.872	
$\text{Ti}_{4c}\text{-O}_{3c}1$ (Å)	1.927	1.812	$\text{Ti}_{4c}\text{-O}_{3c}1$ (Å)	1.936	1.770	
$\text{Ti}_{4c}\text{-O}_{3c}2$ (Å)	1.978	1.844	$\text{Ti}_{4c}\text{-O}_{3c}2$ (Å)	1.950	1.834	
$\text{O}_{2c}1\text{-Ti}_{4c}\text{-O}_{2c}2$ (deg)	172.157	151.292	$\text{O}_{2c}1\text{-Ti}_{4c}\text{-O}_{2c}2$ (deg)	172.157	140.546	

rated Ti_{6c} and O_{3c} . On anatase $\text{TiO}_2(101)$, however, all the rectangular units are closely packed, whereas on brookite $\text{TiO}_2(210)$, rotated rectangular units are closely packed along $[001]$ only. Altogether, brookite $\text{TiO}_2(210)$ looks like a distorted anatase (101) surface. From the relaxed structure shown in Fig. 9(a), and the structural parameters in Table IX, we can also see that the atomic displacements on brookite $\text{TiO}_2(210)$ have trends similar to those on anatase $\text{TiO}_2(101)$.¹⁶ For example, the Ti_{5c} and Ti_{6c} atoms are relaxed inward (~ 0.06 Å) and outward (~ 0.14 Å), respectively, and the topmost O_{3c} [$\text{O}_{3c}1$, Fig. 9(a)] is relaxed outward (~ 0.26 Å).

The computed formation energy of relaxed brookite $\text{TiO}_2(210)$ is 0.70 J m^{-2} , which makes this surface one of the most stable among all the brookite surfaces. However, it is still $\sim 0.26 \text{ J m}^{-2}$ higher than that of anatase $\text{TiO}_2(101)$,²³ probably because of the above described surface distortion.

9. Brookite $\text{TiO}_2(120)$ and (121)

Brookite $\text{TiO}_2(120)$ is a vicinal surface with (010) terraces. The relaxed structure of the (120) termination considered in this work is shown in Fig. 10. It exposes cus Ti_{4c} , Ti_{5c} , and O_{2c} atoms, as well as saturated Ti_{6c} and O_{3c} atoms.

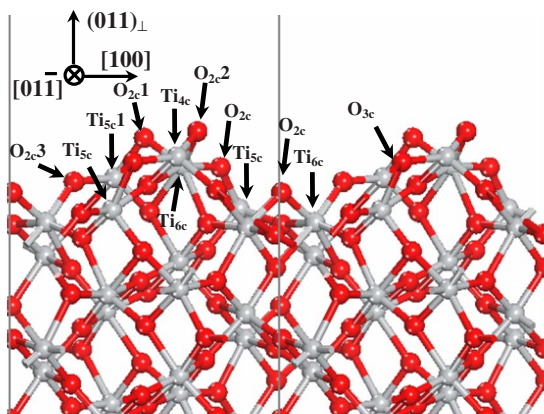


FIG. 6. (Color online) Optimized structure of brookite $\text{TiO}_2(011)$. Atoms in two surface cells are shown (cell boundaries are thin lines in gray). Some of the exposed atoms are named and the directions are given. $(011)_\perp$ indicates the normal of the (011) surface.

Instead, no Ti_{5c} atom is present on the bulk-truncated brookite (010) surface. From the relaxed structure and the structural parameters (see Table X), it appears that the relaxation is significant and very similar to that occurring on the type II brookite (010) surface. For example, the three Ti_{4c} in the unit cell are all relaxed inward (~ 0.1 Å), while the O_{2c} atoms are relaxed outward (~ 0.4 Å). In addition, one of the exposed sixfold (Ti_{6c} , Fig. 10) Ti is relaxed outward by as much as 0.6 Å, so that its bond with the subsurface threefold O is broken (dashed arrow, Fig. 10). The computed surface energy is 0.82 J m^{-2} , slightly higher than that of relaxed brookite $\text{TiO}_2(010)$ (0.77 J m^{-2} , Table I), due to the presence of extra cus Ti atoms (Ti_{5c}) on the (120) surface.

Brookite $\text{TiO}_2(121)$ is another surface that looks very irregular and has several possible terminations. Among them, we chose the one with the lowest cus Ti concentration (not shown), which exposes two Ti_{4c} and five Ti_{5c} in each unit cell. After relaxation, the surface largely keeps its original conformation, even though several surface O atoms relax quite significantly to improve the local configuration of the polyhedra. The computed surface energy is 1.04 J m^{-2} . This rather high value is consistent with the high concentration of exposed cus Ti atoms.

IV. DISCUSSION AND CONCLUSIONS

As pointed out in Sec. III A, there are structural similarities between bulk brookite and the other two TiO_2 polymorphs, rutile and anatase. It is then not surprising that structural similarities do also occur for their surfaces. These are sum-

TABLE VII. Structural parameters of bulk-truncated (before) and optimized (after) brookite $\text{TiO}_2(011)$; surface atoms are indicated as in Fig. 6.

	Brookite $\text{TiO}_2(011)$	
	Before	After
$\text{Ti}_{4c}\text{-O}_{3c}$ (Å)	1.936	1.922
$\text{Ti}_{4c}\text{-O}_{2c}2$ (Å)	1.978	1.816
$\text{Ti}_{5c}1\text{-O}_{2c}1$ (Å)	1.929	1.851
$\text{Ti}_{5c}1\text{-O}_{2c}3$ (Å)	1.950	1.838
$\text{O}_{3c}\text{-Ti}_{4c}\text{-O}_{2c}2$ (deg)	199.032	146.105

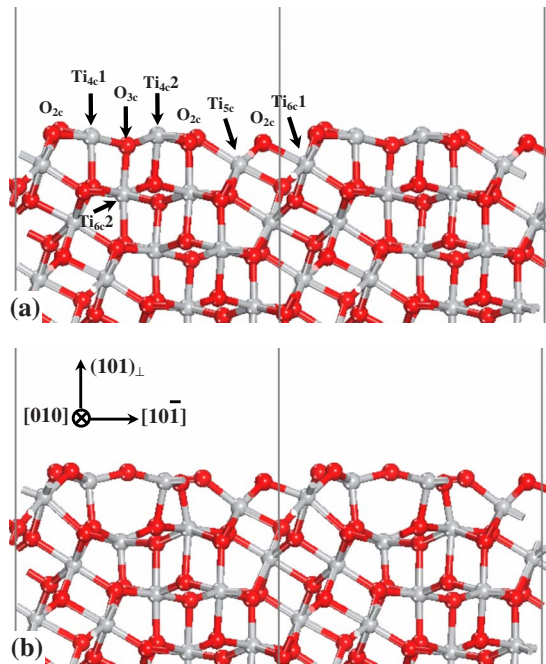


FIG. 7. (Color online) Brookite $\text{TiO}_2(101)$ before (a) and after (b) optimization. Atoms in two surface cells are shown (cell boundaries are thin lines in gray). $(101)_\perp$ indicates the direction normal to the (101) surface.

marized in Table II, where the low-index brookite TiO_2 surfaces and the corresponding rutile and/or anatase surfaces that have similar structures are reported. Since the stacks of TiO_6 octahedra along the c direction ($[001]$) in bulk brookite are very similar to those of rutile (and different from anatase), the brookite surface planes cut through the c axis always have counterparts in rutile; e.g., the brookite (001) and (101) surfaces look quite similar to rutile (011) and (111) , respectively. Moreover, since the stacks of TiO_6 octahedra along the a ($[100]$) and b ($[010]$) directions in bulk brookite have patterns close to those in both rutile and anatase, we can find corresponding rutile and/or anatase surfaces for those brookite surface planes cut through the a and/or b axes.

An analysis of the optimized structures for brookite surfaces shows some general trends in the geometry changes occurring upon relaxation. The most significant one is that the outmost cus Ti atoms, especially the cus Ti with a rather small coordination number, such as Ti_{4c} , always relax inward, while the nearby O atoms they are bonded to relax outward. The cus Ti atoms are usually at protruding positions

TABLE VIII. Structural parameters of bulk-truncated (before) and optimized (after) brookite $\text{TiO}_2(101)$. O'_{3c} and O''_{3c} are the three-fold O atoms bonding with Ti_{4c1} and Ti_{4c2} , respectively, from below. Surface atoms are labeled as in Fig. 7.

Brookite $\text{TiO}_2(101)$		
	Before	After
$\text{Ti}_{4c1}-\text{O}_{3c}$ (Å)	1.927	1.897
$\text{Ti}_{4c2}-\text{O}_{3c}$ (Å)	1.936	1.866
$\text{Ti}_{4c1}-\text{O}'_{3c}$ (Å)	1.987	1.857
$\text{Ti}_{4c2}-\text{O}''_{3c}$ (Å)	1.929	1.855
$\text{Ti}_{6c2}-\text{O}_{3c}$ (Å)	1.929	2.800
$\text{Ti}_{4c1}-\text{O}_{3c}-\text{Ti}_{4c2}$ (deg)	203.082	158.373

and on the face of a $\text{TiO}_x(x<6)$ polyhedron on the bulk-truncated surfaces. The inward relaxation of these atoms, together with the simultaneous outward relaxation of the neighboring O atoms, is a way to compensate for the missing Ti-O bond(s)³⁵ and to bring these cus Ti atoms closer to the center of the polyhedron after optimization.¹

Similar to what is found on other metal oxide surfaces, our results show that the most important factors in determining the stability of brookite surfaces are the coordination and concentration of coordinatively unsaturated atoms, mainly of the cus metal atoms. This is particularly evident in the case of the four possible terminations of brookite $\text{TiO}_2(111)$ (see Sec. III B 7). Our calculations clearly show that the termination with the lowest concentration of cus Ti has the lowest formation energy, while that with the highest cus Ti concentration is the least stable. The relative stabilities of surface terminations with similar concentrations of cus metal atoms are more difficult to predict. In these cases, total energy calculations for the fully relaxed structures are essential. For instance, the brookite $\text{TiO}_2(010)$, (001) , and (110) surfaces have each two terminations whose relative stability is hard to assess without performing total energy calculations. For these surfaces, our results suggest that the structure that is capable to undergo the larger relaxation always has the lower formation energy, as, e.g., in the case of the (001) surface.

Finally, the computed surface formation energies can be used to determine the equilibrium crystal shape of brookite via the Wulff construction.³⁶ As shown in Fig. 11, our calculated shape for brookite exposes seven different facets: (100) , (010) , (001) , (011) , (101) , (111) , and (210) , whose relative contributions to the total area of the crystal are given in Table I. We can see that most of the surface area is taken

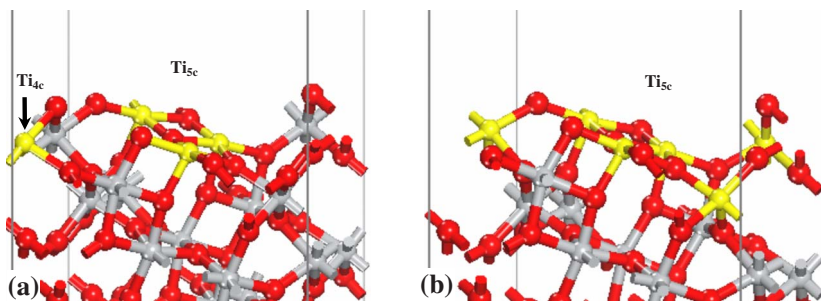


FIG. 8. (Color online) Brookite $\text{TiO}_2(111)$: (a) type I and (b) type II terminations. Exposed cus Ti atoms are highlighted in yellow. The atoms shown belong to a single surface cell.

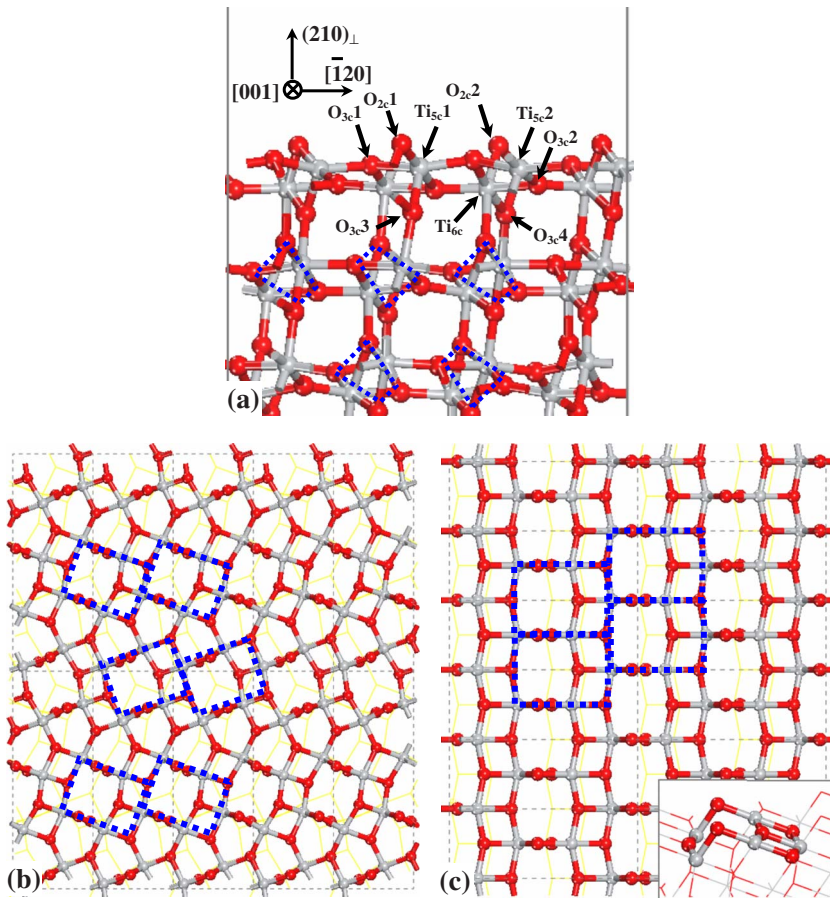


FIG. 9. (Color online) (a) Optimized structure of brookite $\text{TiO}_2(210)$; $(210)_\perp$ indicates the direction normal to the (210) surface. Top view of bulk-truncated (b) brookite $\text{TiO}_2(210)$ and (c) anatase $\text{TiO}_2(101)$; the dashed blue rectangles show that the main building blocks [see also inset in (c)] are similar on the two surfaces.

by the (111) , (210) , (010) , and reconstructed (001) facets. A comparison of this predicted shape with real natural and/or synthetic brookite samples is not straightforward, probably because the observed shapes of “real” brookite samples are influenced by the environmental growth conditions, whereas our calculations refer to surfaces in vacuum. Natural brookite samples show various morphologies, one of the most typical being “tabular on $\{010\}$, striated parallel to $[001]$ and elongated.”³⁷ For synthetic brookite nanocrystals, the shape of nanoplates has been reported.¹¹ In any case, despite some differences between calculated and observed shapes, it appears that the most commonly exposed surfaces in real samples have relatively low formation energies according to our calculations.

TABLE IX. Structural parameters of bulk-truncated (before) and optimized (after) brookite $\text{TiO}_2(210)$; surface atoms are labeled as in Fig. 9.

	Brookite $\text{TiO}_2(210)$	
	Before	After
$\text{Ti}_{5c1}-\text{O}_{2c1}$ (Å)	1.987	1.812
$\text{Ti}_{5c2}-\text{O}_{2c2}$ (Å)	1.929	1.806
$\text{Ti}_{5c1}-\text{O}_{3c1}$ (Å)	1.978	1.998
$\text{Ti}_{5c1}-\text{O}_{3c3}$ (Å)	1.927	1.784
$\text{Ti}_{5c2}-\text{O}_{3c2}$ (Å)	1.987	2.009
$\text{Ti}_{5c2}-\text{O}_{3c4}$ (Å)	1.978	1.808

From the results in Table I, we can also evaluate the average surface energy $\langle\gamma_B\rangle$ of a brookite sample, for which we obtain $\langle\gamma_B\rangle=0.71 \text{ J/m}^2$. This value has not an absolute meaning since it depends sensitively on a few computational details, notably the specific DFT functional and the pseudo-potential used.²³ However, this $\langle\gamma_B\rangle$ can be directly compared to the average surface energy of $\sim 0.5 \text{ J/m}^2$, which we previously obtained for an anatase crystal^{16,23} since the calculations in those works were performed with the same computational setup used in this paper. Interestingly, the relative surface energy values of brookite vs anatase that we find

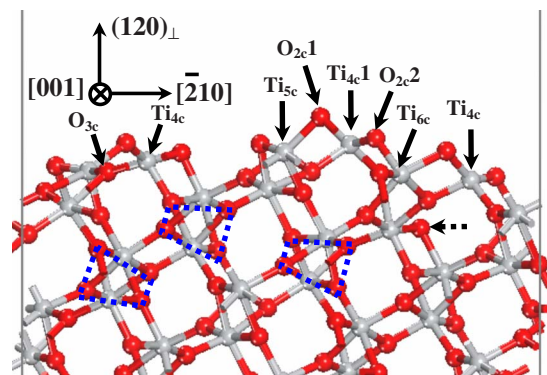


FIG. 10. (Color online) Optimized structure of brookite $\text{TiO}_2(120)$. $(120)_\perp$ indicates the direction normal to the (120) surface.

TABLE X. Structural parameters of bulk-truncated (before) and optimized (after) brookite $\text{TiO}_2(120)$. Surface atoms are indicated as in Fig. 10.

	Brookite $\text{TiO}_2(120)$	
	Before	After
$\text{Ti}_{4c}1\text{-O}_{2c}1$ (Å)	1.929	1.841
$\text{Ti}_{4c}1\text{-O}_{2c}2$ (Å)	1.987	1.862
$\text{Ti}_{5c}\text{-O}_{2c}1$ (Å)	1.936	1.878
$\text{Ti}_{6c}\text{-O}_{2c}2$ (Å)	1.950	1.810
$\text{O}_{2c}1\text{-Ti}_{4c}1\text{-O}_{2c}2$ (deg)	172.157	138.604

agree remarkably well with the experimental values obtained by Ranade *et al.*³⁰ from the crossover in stability of nanophase TiO_2 polymorphs, despite the incorrect ordering of the different TiO_2 bulk phases predicted by DFT (see Sec. III A),

In conclusion, in this work we have presented comprehensive first-principles calculations of low-index stoichiometric brookite TiO_2 surfaces corresponding to ten different lattice planes. On the basis of the computed surface formation energies, we have determined the equilibrium crystal shape of brookite and estimated its average surface energy. This is found to be higher than the similarly estimated average surface energy for an anatase crystal, in agreement with experimental results on the stability and phase transformations of TiO_2 nanoparticles.³⁰ As a final remark, we point out that despite the structural similarities between the surfaces of brookite and those of rutile and anatase, their electronic and chemical properties can be significantly different. Notably, in a preliminary comparative study of the electronic densities of

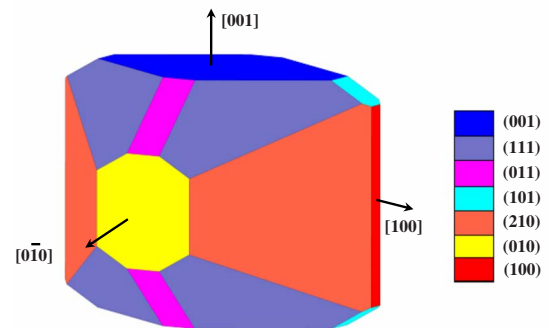


FIG. 11. (Color online) Equilibrium crystal shape of brookite TiO_2 , as obtained through the Wulff construction. Different facets have different colors, and the orientations are given.

states of brookite $\text{TiO}_2(210)$ and anatase $\text{TiO}_2(101)$, we have found differences suggesting that their chemical reactivities may not be the same.³⁸ With this work, we hope to provide results that will be useful for studies of titania phase transformations and for future investigations of the chemistry of brookite surfaces as well.

ACKNOWLEDGMENTS

The authors acknowledge the financial support from the Department of Energy Office of Science (Grant No. DE-FG02-05ER15702) and the computing time at Princeton Institute for Computational Science and Engineering, TIGRESS High Performance Computing Center at Princeton University, and the Chemistry Department.

*Present address: Research Institute of Industrial Catalysis, East China University of Science and Technology, 130 Meilong Road, Shanghai 200237, People's Republic of China.

¹U. Diebold, *Surf. Sci. Rep.* **48**, 53 (2003).

²U. Diebold, N. Ruzycski, G. S. Herman, and A. Selloni, *Catal. Today* **85**, 93 (2003).

³A. Hagfeldt and M. Grätzel, *Chem. Rev. (Washington, D.C.)* **95**, 49 (1995).

⁴A. L. Linsebigler, G. Q. Lu, and J. T. Yates, Jr., *Chem. Rev. (Washington, D.C.)* **95**, 735 (1995).

⁵R. L. Penn and J. F. Banfield, *Am. Mineral.* **83**, 1077 (1998).

⁶S. L. Isley and R. L. Penn, *J. Phys. Chem. B* **110**, 15134 (2006).

⁷K. Tomita, V. Petrykin, M. Kobayashi, M. Shiro, M. Yoshimura, and M. Kakihana, *Angew. Chem., Int. Ed.* **45**, 2378 (2006).

⁸A. Di Paola, M. Addamo, M. Bellardita, E. Cazzanelli, and L. Palmisano, *Thin Solid Films* **515**, 3527 (2007).

⁹M. A. Reddy, M. S. Kishore, V. Pralong, U. V. Varadaraju, and B. Raveau, *Electrochem. Solid-State Lett.* **10**, A29 (2007).

¹⁰M. Addamo, M. Bellardita, A. Di Paola, and L. Palmisano, *Chem. Commun. (Cambridge)* **2006**, 4943.

¹¹J. G. Li, T. Ishigaki, and X. D. Sun, *J. Phys. Chem. C* **111**, 4969 (2007).

¹²W. F. Yan, B. Chen, S. M. Mahurin, S. Dai, and S. H. Overbury, *Chem. Commun. (Cambridge)* **2004**, 1918.

¹³T. Shibata, H. Irie, M. Ohmori, A. Nakajima, T. Watanabe, and K. Hashimoto, *Phys. Chem. Chem. Phys.* **6**, 1359 (2004).

¹⁴W. F. Yan, B. Chen, S. M. Mahurin, V. Schwartz, D. R. Mullins, A. R. Lupini, S. J. Pennycook, S. Dai, and S. H. Overbury, *J. Phys. Chem. B* **109**, 10676 (2005).

¹⁵S. Bakardjieva, V. Stengl, L. Szatmary, J. Subrt, J. Lukac, N. Murafa, D. Niznansky, K. Cizek, J. Jirkovsky, and N. Petrova, *J. Mater. Chem.* **16**, 1709 (2006).

¹⁶M. Lazzeri, A. Vittadini, and A. Selloni, *Phys. Rev. B* **63**, 155409 (2001).

¹⁷X. Q. Gong and A. Selloni, *J. Phys. Chem. B* **109**, 19560 (2005).

¹⁸X. Q. Gong, A. Selloni, and A. Vittadini, *J. Phys. Chem. B* **110**, 2804 (2006).

¹⁹O. Bikondoa, C. L. Pang, R. Ithnin, C. A. Muryn, H. Onishi, and G. Thornton, *Nat. Mater.* **5**, 189 (2006).

²⁰D. Matthey, J. G. Wang, S. Wendt, J. Matthesen, R. Schaub, E. Laegsgaard, B. Hammer, and F. Besenbacher, *Science* **315**, 1692 (2007).

²¹X.-Q. Gong and A. Selloni, *J. Catal.* **249**, 134 (2007).

²²K. Reuter and M. Scheffler, *Phys. Rev. B* **68**, 045407 (2003).

- ²³X. Q. Gong, A. Selloni, M. Batzill, and U. Diebold, *Nat. Mater.* **5**, 665 (2006).
- ²⁴A. Beltran, L. Gracia, and J. Andres, *J. Phys. Chem. B* **110**, 23417 (2006).
- ²⁵M. Posternak, A. Baldereschi, E. J. Walter, and H. Krakauer, *Phys. Rev. B* **74**, 125113 (2006).
- ²⁶J. P. Perdew, K. Burke, and M. Ernzerhof, *Phys. Rev. Lett.* **77**, 3865 (1996).
- ²⁷S. Baroni, S. De Gironcoli, A. Dal Corso, and P. Giannozzi, QUANTUM-ESPRESSO, <http://www.democritos.it>
- ²⁸D. Vanderbilt, *Phys. Rev. B* **41**, 7892 (1990).
- ²⁹R. W. G. Wyckoff, *Crystal Structures* (Interscience, New York, 1963).
- ³⁰M. R. Ranade, A. Navrotsky, H. Z. Zhang, J. F. Banfield, S. H. Elder, A. Zaban, P. H. Borse, S. K. Kulkarni, G. S. Doran, and H. J. Whitfield, *Proc. Natl. Acad. Sci. U.S.A.* **99**, 6476 (2002).
- ³¹J. Muscat, V. Swamy, and N. M. Harrison, *Phys. Rev. B* **65**, 224112 (2002).
- ³²F. Labat, P. Baranek, C. Domain, C. Minot, and C. Adamo, *J. Chem. Phys.* **126**, 154703 (2007).
- ³³M. Ramamoorthy, D. Vanderbilt, and R. D. King-Smith, *Phys. Rev. B* **49**, 16721 (1994).
- ³⁴R. Lindsay, A. Wander, A. Ernst, B. Montanari, G. Thornton, and N. M. Harrison, *Phys. Rev. Lett.* **94**, 246102 (2005).
- ³⁵X. L. Yin, R. Miura, A. Endou, I. Gunji, R. Yamauchi, M. Kubo, A. Stirling, A. Fahmi, and A. Miyamoto, *Appl. Surf. Sci.* **119**, 199 (1997).
- ³⁶G. Wulff, *Z. Kristallogr. Mineral.* **34**, 449 (1901).
- ³⁷PRISMATIC {120}, modified, Ural Leuchtenberg, 1872, in V. M. Goldschmidt, *Atlas der Krystallformen* (Winter, Heidelberg, 1913).
- ³⁸W. K. Li, G. Lu, X. Q. Gong, and A. Selloni (to be submitted).